(1)

ARL-TR-92-29

Copy No. 66

Depth Dependence of the Single and Triple Traversal Correlation Trace

Technical Report under Contract N00039-91-C-0082,
TD No. 01A1030, Spectral/Temporal Signal and Noise Analysis

Elizabeth L. Miller
Evan K. Westwood

Applied Research Laboratories
The University of Texas at Austin
P. O. Box 8029 Austin, TX 78713-8029

24 November 1992

Technical Report

Prepared for:
Naval Command Control and Ocean Surveillance Center
RDT&E Division
San Diego, CA 92152-5000

Monitored by:
Space and Naval Warfare Systems Command
Department of the Navy
Washington, D.C. 20363-5100

UNCLASSIFIED

REPORT DOCUMENTATION PAGE	Form Approved OMB No 0704 0188

AGENCY USE ONLY (Leave blank)	2. REPORT DATE	3. REPORT TYPE AND DATES COVERED
	24 Nov 92	technical report

TITLE AND SUBTITLE	5. FUNDING NUMBERS
Depth Dependence of the Single and Triple Traversal Correlation Trace Technical Report under Contract N00039-91-C-0082, TD No. 01A1030, Spectral/Temporal Signal and Noise Analysis	N00039-91-C-0082 TD No. 01A1030
AUTHOR(S) Miller, Elizabeth L., Westwood, Evan K.	
PERFORMING ORGANIZATION NAME(S) AND ADDRESS(ES) Applied Research Laboratories The University of Texas at Austin P. O. Box 8029 Austin, Texas 78713-8029	8. PERFORMING ORGANIZATION REPORT NUMBER ARL-TR-92-29
SPONSORING/MONITORING AGENCY NAME(S) AND ADDRESS(ES) Naval Command Control and Ocean Surveillance Center RDT&E Division San Diego, CA 92152-5000 Space and Naval Warfare Systems Command Department of the Navy Washington, DC 20363-5100	10. SPONSOR/MONITORING AGENCY REPORT NUMBER

11. SUPPLEMENTARY NOTES

12a. DISTRIBUTION/AVAILABILITY STATEMENT	12b. DISTRIBUTION CODE
Approved for public release; distribution is unlimited.	

13. ABSTRACT (Maximum 200 words)

Experimental evidence of the dependence on source depth of a particular correlation trace measured at near-bottom sensors in deep water is presented. The depth-dependent trace is produced by eigenrays having one and three ocean traversals, i.e., the direct path and the first bottom-bounce rays. A 65-95 Hz pseudo-random noise source towed at 100 m depth during the TAGEX87 experiment is used to examine the correlation trace for submerged sources, while the tow ship itself is used for surface sources. Ray model simulations accurately predict the change in the correlation traces as a function of source depth.

14. SUBJECT TERMS	15. NUMBER OF PAGES
source depth, correlation	28
	16. PRICE CODE

17. SECURITY CLASSIFICATION OF REPORT	18. SECURITY CLASSIFICATION OF THIS PAGE	19. SECURITY CLASSIFICATION OF ABSTRACT	20. LIMITATION OF ABSTRACT
UNCLASSIFIED	UNCLASSIFIED	UNCLASSIFIED	SAR

This page intentionally left blank.

TABLE OF CONTENTS

This page intentionally left blank.

LIST OF FIGURES

This page intentionally left blank.

1. INTRODUCTION

It has been suggested that the width of the correlation trace produced by acoustic rays traversing the ocean once and those traversing it three times (Fig. 1.1) depends on the depth of the source.[1] The TAGEX87 experiment had two suitable sources to test this hypothesis: (1) a pseudo-random noise (PRN) source at a depth of 100 m towed at 5 m/s, and (2) the tow ship itself which generated broadband noise from 0 to 150 Hz. The 65 to 95 Hz PRN source repeated every 0.75 s. There was also a 34 Hz towed source which could be filtered out. To analyze the PRN source and the ship noise separately, correlations were made using the filters shown in Fig. 1.2. Filter 1 retains only those frequencies produced by the PRN source. Filter 2 retains only frequencies higher than those produced by the towed sources.

The TAGEX87 exercise took place in deep water (4625 m) with the sound velocity profile shown in Fig. 1.3. The array used to collect the data consisted of 24 hydrophones spaced 10 m apart with the bottommost hydrophone 41 m off the ocean floor. In the data analyzed, the ship started about 7.56 km from the array (Fig. 1.4), crossed over it, and went out another 42 km. Then, it returned along the same path to about 13 km from the array.

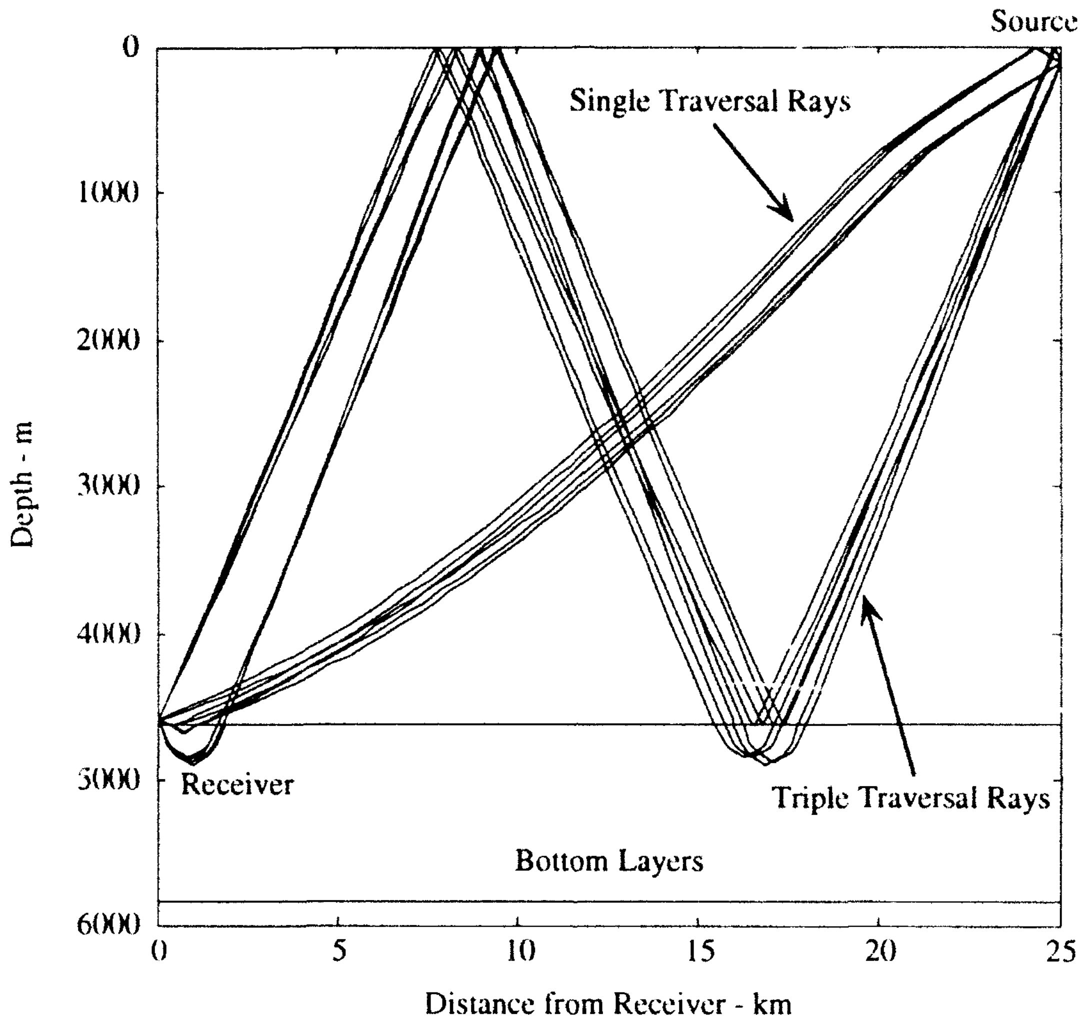

FIG. 1.1 Single and triple traversal rays.

AS-92-666

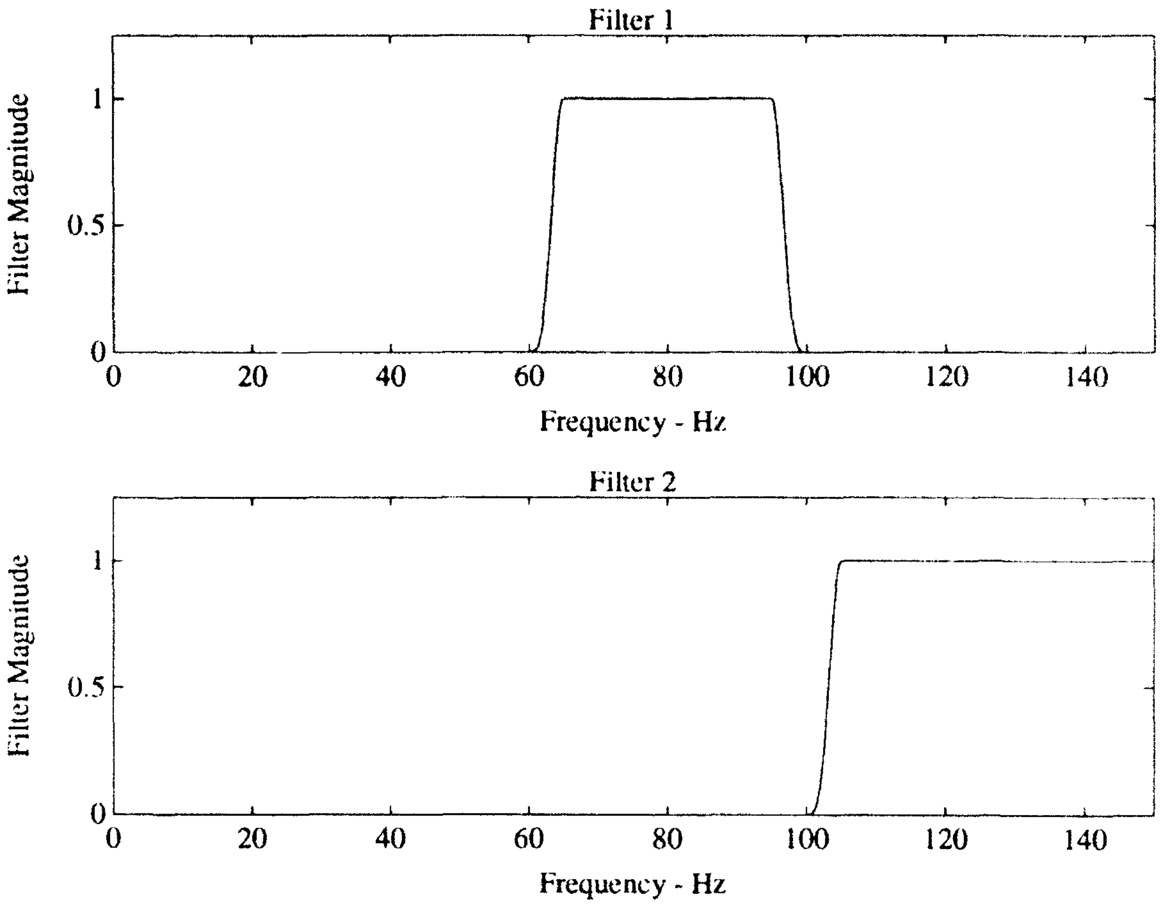

FIG. 1.2 Filters used to analyze data. Filter 1 includes the frequencies produced by the PRN source. Filter 2 excludes frequencies produced by the PRN and 34 Hz sources.

AS-92-667

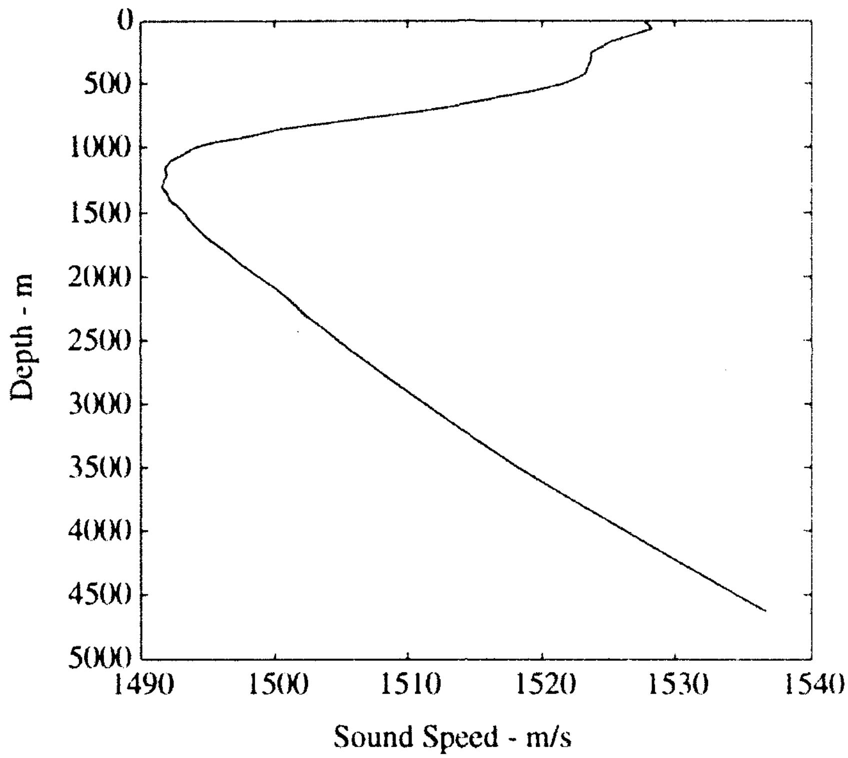

FIG. 1.3 Sound velocity profile for the TAGEX87 experiment.

AS-92-668

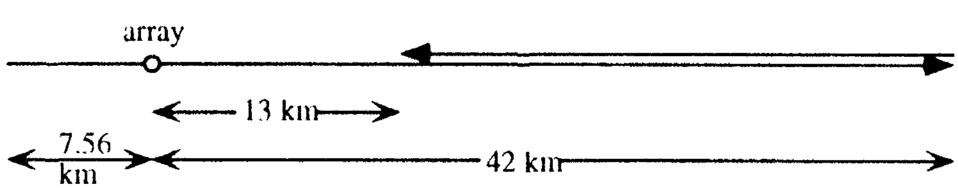

FIG. 1.4 Path of the ship in the TAGEX87 data.

AS-92-669

2. MEASURED 1x3 CORRELATION TRACES

To intensify the correlation between the single and triple traversal rays, it was necessary to beamform the data. Steering angles for the array were taken from the plots of measured noise directionality shown in Fig. 2.1. These plots of beam power versus range and angle were produced by an adaptive beamformer. Positive angles arrive from above, negative from below. For frequencies between 65 and 95 Hz (Fig. 2.1(a)), arrival angles for rays from the PRN source can be determined for one, three, and five-traversal acoustic rays. Only single and triple traversal arrival angles can be obtained for the higher frequency band of 100-150 Hz (Fig. 2.1(b)). The dark regions in the center of the beam noise displays are due to distant ship noise, which arrives nearly horizontally. The vertical line at 30° in the bottom plot is apparently produced by a stationary noise source. The rays with negative arrival angles were weaker due to absorption in the ocean bottom, especially for frequencies above 100 Hz. For this reason, beamforming was performed using positive arrival angles. The noise directionality plots were also used to choose a section of the data in which both the single and triple traversal rays should be detectable.

Using all 24 receivers, two beams were steered that tracked the single and triple traversal ray arrivals. The complex beamformer outputs for the two ray arrivals were then cross-correlated using an envelope correlation and a phase transform. Mu-law mapping was used to intensify Fig. 2.2(a). The resulting correlations are shown in Fig. 2.2. Filter 1 and filter 2 were used to produce Fig. 2.2(a) and Fig. 2.2(b), respectively. The 0.75 s repetition rate of the PRN source results in multiple correlation traces separated by 0.75 s in Fig. 2.2(a). The vertical line in Fig. 2.2(b) is due to the source appearing at 38° in Fig. 2.1(b). It is evident from Fig. 2.2 that the 1x3 correlation trace generated by the PRN is broad along the time delay axis and actually consists of several traces side by side, whereas the trace generated by the ship is narrower and consists of just a single trace.

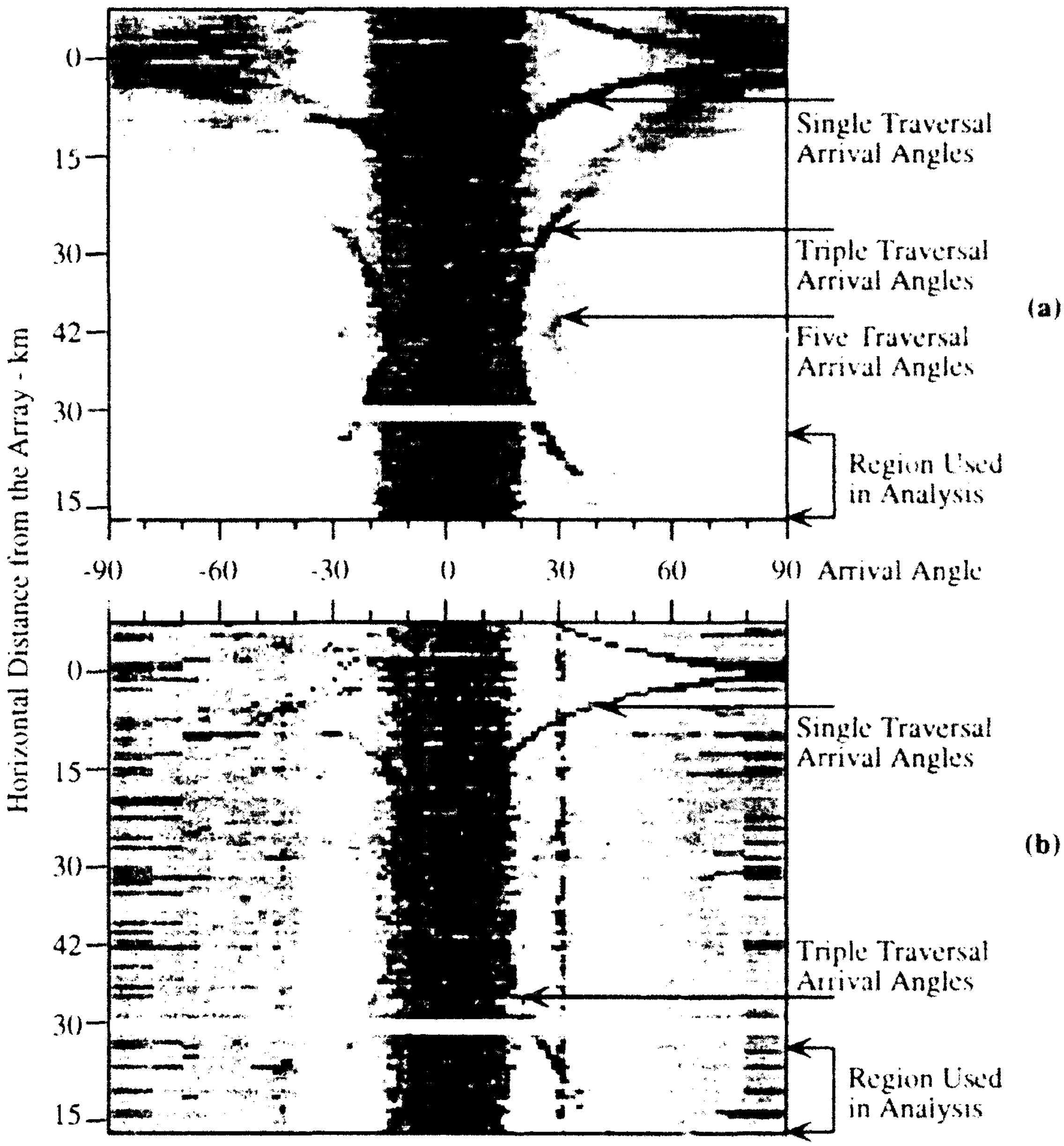

FIG. 2.1 Noise directionality plots for the TAGEX87 data with (a) frequencies between 65 and 95 Hz, and (b) frequencies between 100 and 150 Hz.

AS-92-670

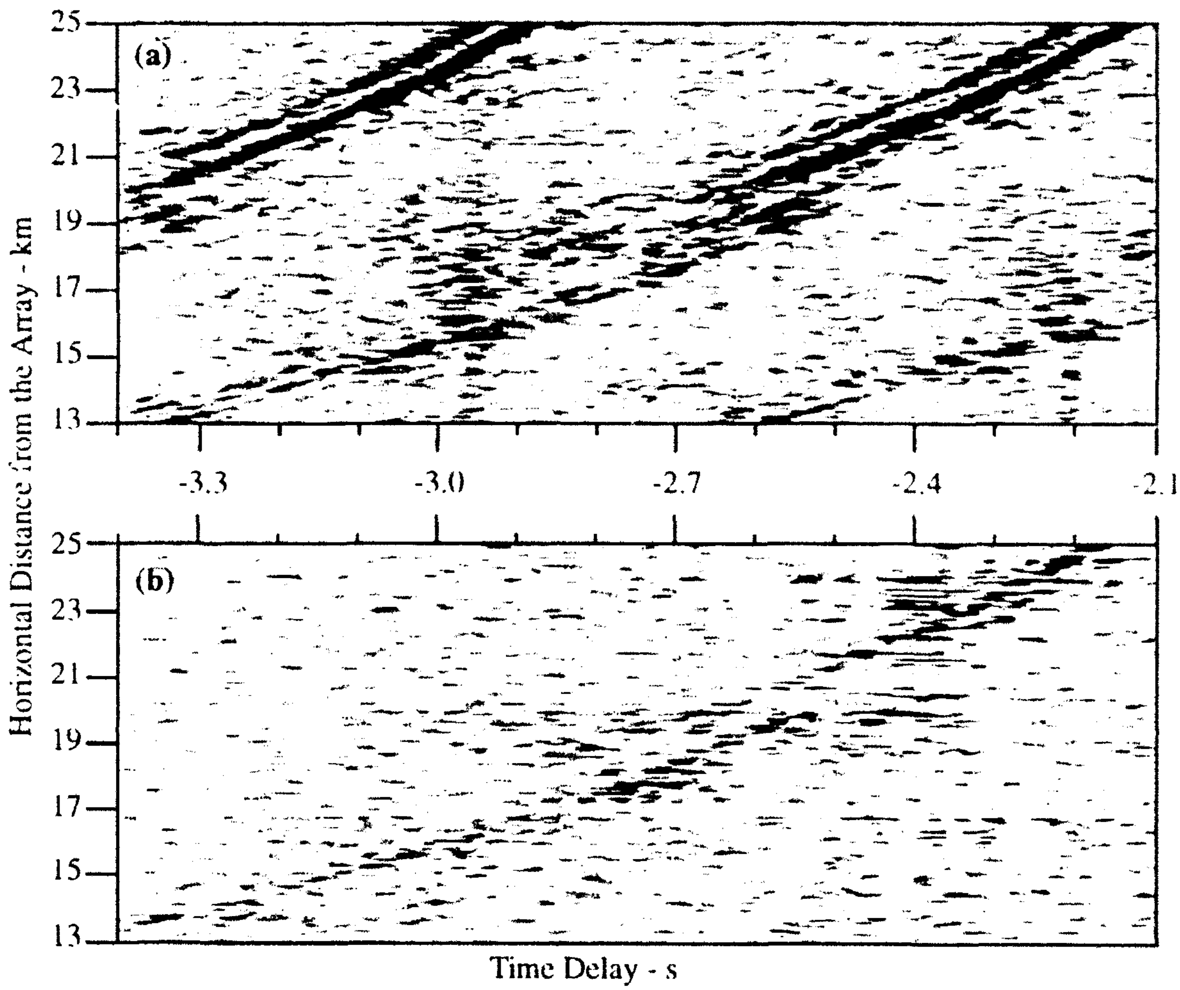

FIG. 2.2 Correlations of TAGEX87 data: (a) PRN source and (b) ship noise.

AS-92-671

This page intentionally left blank.

3. SIMULATED 1x3 CORRELATION TRACES

To investigate the depth dependence of the 1x3 correlation trace, simulations of the correlagrams in Fig. 2.2 were performed. A ray model was used to produce simulated received spectra at the 24 receivers due to an impulsive source. An impulsive source was used for convenience. Any non-repeating broadband signal would result in correlations similar to the ones shown here. Source depths of 5 m and 100 m were simulated. The simulated received spectra were beamformed and crosscorrelated in the same manner as the TAGEX87 data. The resulting correlations are shown in Fig. 3.1. Figures 3.1(a) and 3.1(b) use filter 1, and Figs. 3.1(c) and 3.1(d) use filter 2. In both cases, the deeper simulated source results in a double trace that is wider along the time delay axis. It is clear that the simulated traces for the 100 m source depth (Figs. 3.1(b) and 3.1(d)) are in excellent agreement with the trace produced by the PRN (Fig. 2.2(a)), and that the simulated traces for the 5 m source depth (Figs. 3.1(a) and 3.1(c)) agree with the trace produced by the ship (Fig. 2.2(b)). In addition, it is clear that the width difference in Fig. 2.2 is caused by the change in source depth and not by the filters used.

It is interesting to note the reason for the shift in the simulated traces that occurs at a range of 17 km in Fig. 3.1. The three-traversal rays included in the beamformed simulations are shown arriving from ranges of 16 and 20 km in Fig. 3.2. At the longer range, the strongest ray is the bottom penetrating ray. At shorter ranges, the bottom penetrating ray has a much greater distance to travel through the bottom layers and loses more energy due to absorption. Therefore, at shorter ranges, the specularly reflected ray becomes dominate, and the simulated 1x3 trace undergoes a shift along the time delay axis. Such a shift can also be observed in the measured 1x3 trace of Figs. 2.2 and 4.3(a).

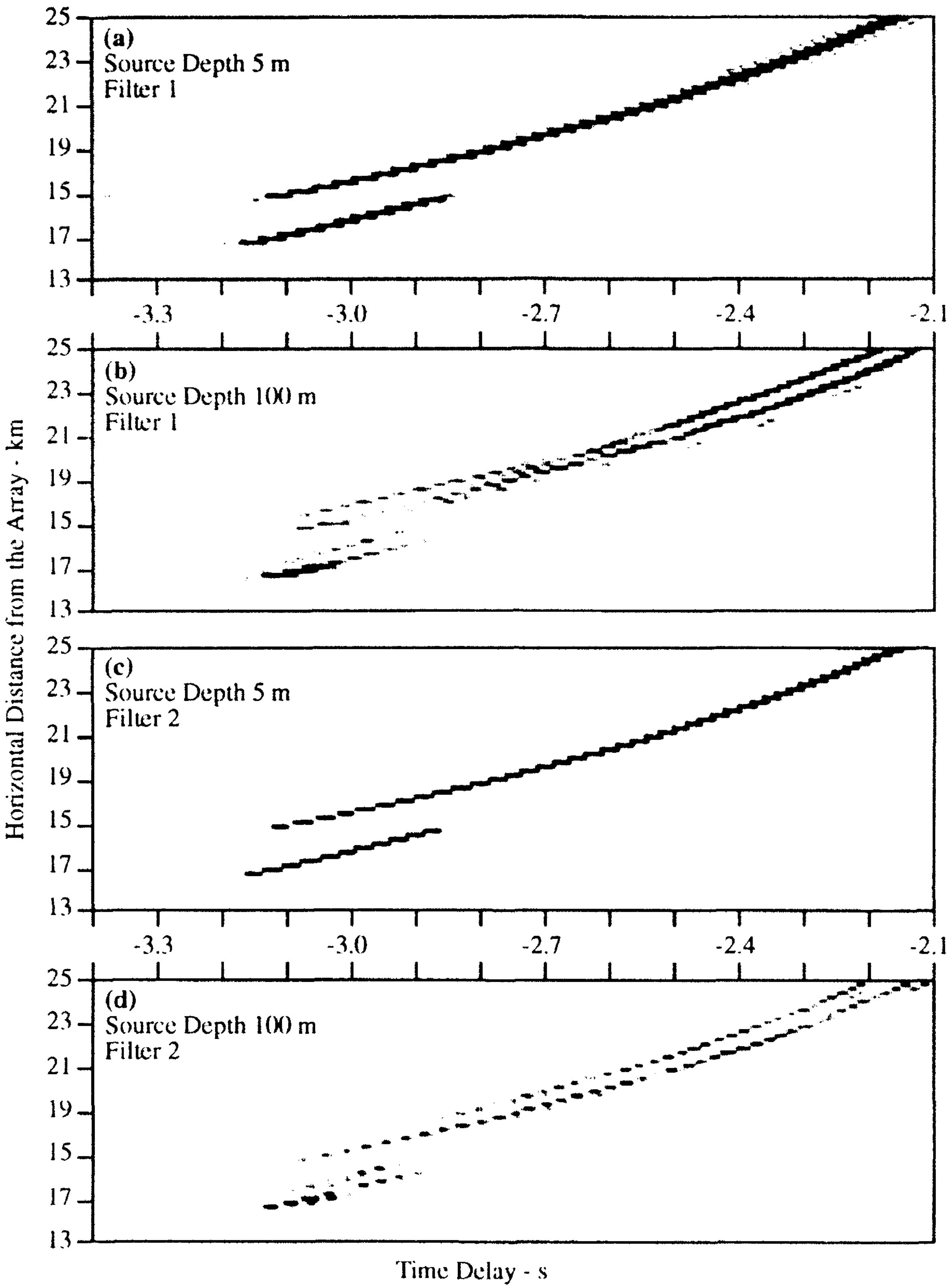

FIG. 3.1 Correlations of simulated sources at 5 m and 100 m depths using the filters shown in Fig. 1.2. White represents a correlation of 0 and black, a correlation of 0.5 or greater.

AS-92-672

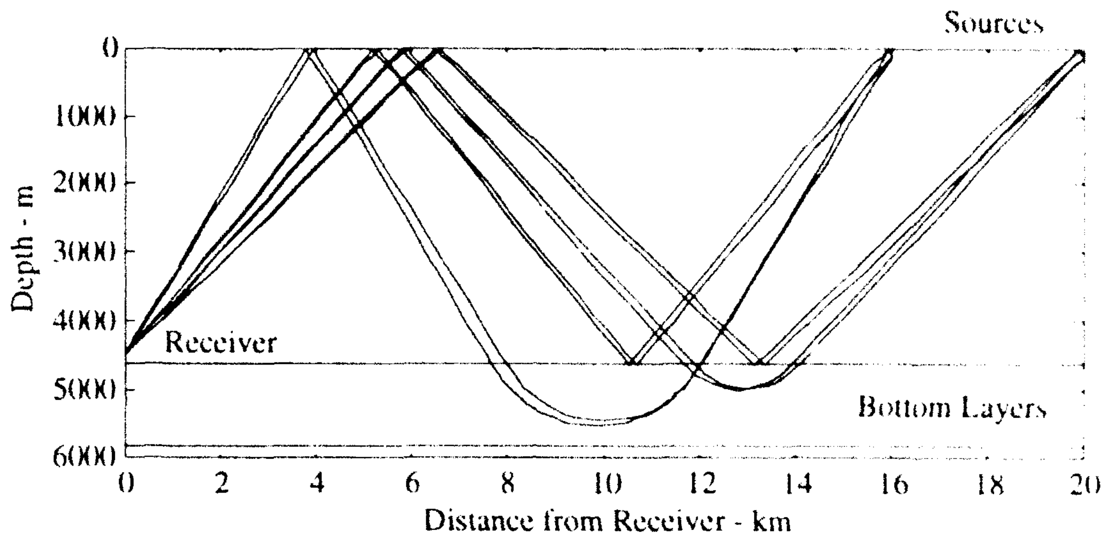

FIG. 3.2 Three-traversal rays included in the beamformed simulations arriving from 16 and 20 km.

AS-92-673

This page intentionally left blank.

4. ANALYSIS OF A SECOND SHIP PASSAGE

Confirming evidence for the depth dependence of the 1x3 trace has been found in another event recorded at the vertical array. A ship moving at 7.2 m/s passed within 800 m of the array. Figure 4.1 shows the ship track. This second event allows us to examine correlation traces produced by a surface source without any possibility of interference from submerged sources. Steering angles obtained from the beam noise plots in Fig. 4.2 were used to beamform the data. The resulting correlations appear in Fig. 4.3. The correlations of Fig. 4.3 are inverted with respect to those of Fig. 2.2 and Fig. 3.1 because the ship was moving away from the array. Like Fig. 2.2, Fig. 4.3(a) used filter 1, and Fig. 4.3(b) used filter 2. The fact that using the narrow PRN filter neither widens the trace nor creates a double trace indicates once again that varying the source depth results in different trace widths.

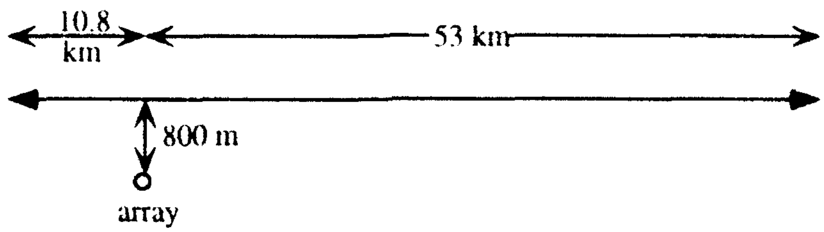

FIG. 4.1 Ship track for the second event.

AS-92-674

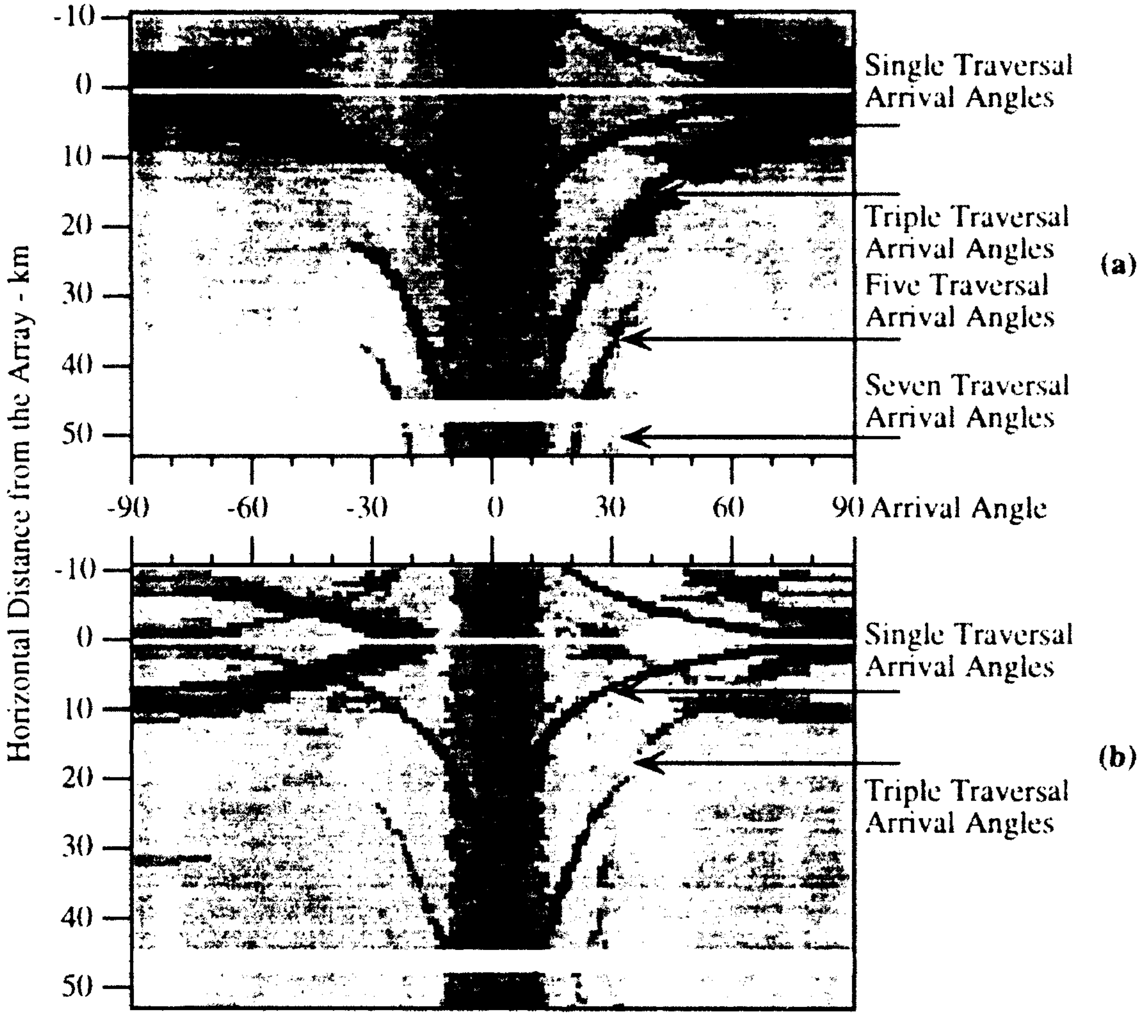

FIG. 4.2 Noise directionality plots for the second event with (a) frequencies between 65 and 95 Hz, and (b) frequencies between 100 and 150 Hz.

AS-92-675

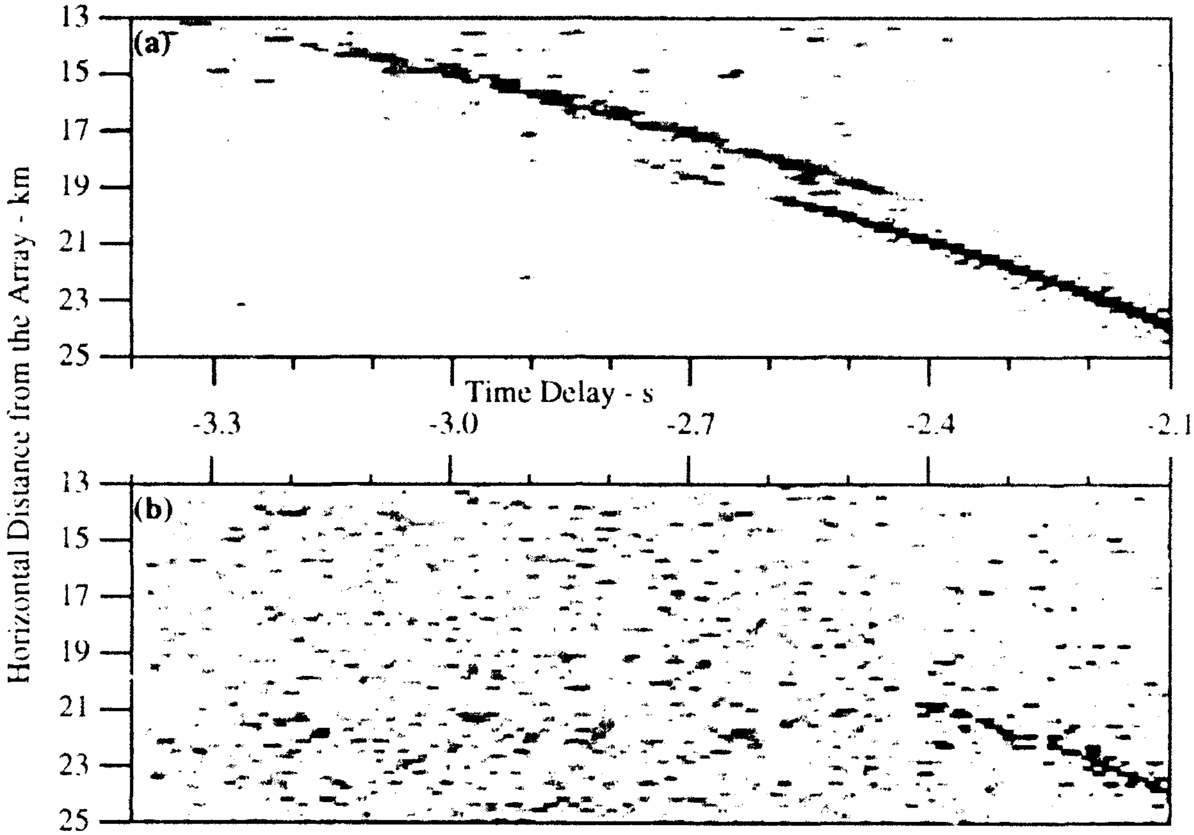

FIG. 4.3 Correlations of second event data. Filter 1 was used to generate (a), and filter 2 was used for (b).

AS-92-676

This page intentionally left blank.

5. CONCLUSION

In conclusion, variation in source depth results in a variation in the 1x3 trace width. A surface source produces a narrow trace. A submerged source produces a trace that is wider along the time delay axis and is actually composed of several traces. As a result, the 1x3 trace can be used to differentiate between a surface and a submerged source.

This page intentionally left blank.

REFERENCES

1. E. K. Westwood, "Broadband Modeling of an FDS Testbed Event: Determination of Source Depth and Track from Lofargrams and Correlagrams (U)," Applied Research Laboratories Technical Report No. 91-10 (ARL-TR-91-10) (SECRET), Applied Research Laboratories, The University of Texas at Austin.

This page intentionally left blank.

24 November 1992

DISTRIBUTION LIST FOR
ARL-TR-92-29
Technical Report Under Contract N00039-91-C-0082
TD No. 01A1030, Spectral/Temporal Signal and Noise Analysis

Copy No.	
	Director
	Naval Command Control and Ocean Surveillance Center
	RDT&E Division
	San Diego, CA 92152-5000
1	Attn: L. Arndt (Code 72)
2	D. Barbour (Code 733)
3	A. D'Amico (Code 734)
4	H. Bucker (Code 541)
5	J. Ehlers (Code 714)
6	D. Hanna (Code 705)
7	J. Lockwood (Code 734)
8	M. Morrison (Code 705)
9	C. Persons (Code 732)
10	K. Rogers (Code 714)
11	H. Schenck (Code 701)
	Commander
	Space and Naval Warfare Systems Command
	Department of the Navy
	Washington, D.C. 20363-5100
12	Attn: CAPT K. Evans (PD80)
13	C. Andriani (PD80T)
14	L. Parish (PMW181T)
15	CDR S. Hollis (PMW182)
16	G. Hetland (PMW183-34)
17	L. Fabian (PMW183-4)
18	W. Richter (PMW183-41)
19	M. Potosky (PMW183-11)
20	R. Hobart (PMW184)
21	CAPT W. Hatcher (PD80D)
22	LCDR S. Kasputis (PMW184T)
23	LCDR P. Feldman (PMW 183-113)
	Office of the Assistant Secretary of the Navy
	(Research, Development, and Acquisition)
	Department of the Navy
	Washington, DC 20350-1000
24	Attn: G. Cann

Distribution List for ARL-TR-92-29 under Contract N00039-91-C-0082, TD No. 01A1030 (cont'd)

<u>Copy No.</u>

Office of the Deputy Assistant Secretary of the Navy
Antisubmarine Warfare Programs
Department of the Navy
Washington, DC 20350-1000
25 Attn: A. Bisson
26 CDR D. Backes

Office of the Chief of Naval Operations
Department of the Navy
Washington, D.C. 20350-2000
27 Attn: J. Schuster (N87T)
28 CAPT F. Crawford (N874)

Office of the Chief of Naval Operations
Naval Observatory
34th and Massachusetts Ave.
Washington, D.C. 20390
29 Attn: R. Winokur (Code 096T)

Office of the Chief of Naval Research
Department of the Navy
Arlington, VA 22217-5000
30 Attn: R. Feden (Code 124A)
31 B. Blumenthal (Code 124A)

Office of the Chief of Naval Research
Office of Naval Technology
Department of the Navy
Arlington, VA 22217-5000
32 Attn: A. Faulstich (ONT23)
33 CAPT R. Fitch (ONT23D)
34 R. Doolittle (ONT230)
35 T. Goldsberry (ONT231)
36 C. Votaw (ONT234)

Commanding Officer
Naval Research Laboratory
Washington, DC 20375-5000
37 Attn: D. Bradley (Code 5100)
38 S. Wolf (Code 5160)

Distribution List for ARL-TR-92-3 under Contract N00039-91-C-0082, TD No. 01A1030 (cont'd)

Copy No.

Commanding Officer
Naval Research Laboratory
Stennis Space Center, MS 39529-5004

39 Attn: E. Chaika (Code 124A)
40 B. Adams (Code 110A)
41 J. Matthews (Code 222)
42 D. Del Balzo (Code 244)
43 R. Wagstaff (Code 425)
44 H. Ali (Code 425)

Defense Advanced Research Projects Agency
3701 N. Fairfax Drive
Arlington, VA 22203-1714

45 Attn: C. Stuart
46 W. Carey

Commander
Naval Air Systems Command
Department of the Navy
Washington, D.C. 20361-7121

47 Attn: E. Benson (PMA 264)

Commander
Naval Surface Weapons Center, Dahlgren Division
Silver Spring, MD 20903-5000

48 Attn: M. Stripling

Commander
Carderock Division
Naval Surface Warfare Center
Bethesda, MD 20084-5001

49 Attn: Library

Commanding Officer
Naval Oceanographic Office
Stennis Space Center, MS 39522-5001

50 Attn: W. Jobst (Code 7300)
51 R. Hecht (Code 7310)
52 CDR R. Houtman (NESPO)

Distribution List for ARL-TR-92-29 under Contract N00039-91-C-0082, TD No. 01A1030 (cont'd)

Copy No.

	Commanding Officer Naval Air Warfare Center Aircraft Division, Warminster Warminster, PA 18974-5000	
53	Attn:	L. Allen
54		C. Bartberger
55		B. Steinberg (Code 5031)
	Commander Naval Undersea Warfare Center Division New London, CT 06320-5594	
56	Attn:	B. Cole (Code 33A)
57		F. DiNapoli
58		P. Herstein (Code 33A3)
59		T. Bell
60		E. Jensen (Code 3332)
61		R. Davenport (Code 3332)
	Commander Naval Undersea Warfare Center Division Newport, RI 02841-5047	
62	Attn:	E. Sullivan (Code 103)
	Superintendent Naval Postgraduate School Monterey, CA 93940	
63	Attn:	Library
	Commanding Officer Coastal Systems Station, Dahlgren Division Naval Surface Warfare Center Panama City, FL 32407-5000	
64	Attn:	G. McLeroy
	Commanding Officer Naval Intelligence Activity Washington, D.C. 20395	
65	Attn:	E. McWethy (NAVMIC-DI56)
66	Commanding Officer and Director Defense Technical Information Center Cameron Station, Building 5 5010 Duke Street Alexandria, VA 22314	

Distribution List for ARL-TR-92-3 under Contract N00039-91-C-0082, TD No. 01A1030 (cont'd)

Copy No.

Director
North Atlantic Treaty Organization
SACLANT ASW Research Centre
APO New York 09019

67 Attn: Library
68 F. Jensen
69 T. Akal

Applied Physics Laboratory
The Johns Hopkins University
Johns Hopkins Road
Laurel, MD 20810

70 Attn: J. Lombardo
71 A. Boyles
72 K. McCann

Applied Research Laboratory
The Pennsylvania State University
P.O. Box 30
State College, PA 16801

73 Attn: S. McDaniel
74 D. McCammon

Marine Physical Laboratory
Scripps Institution of Oceanography
The University of California, San Diego
San Diego, CA 92132

75 Attn: F. Fisher
76 V. Anderson
77 W. Hodgkiss

Scripps Institution of Oceanography
The University of California, San Diego
La Jolla, CA 92037

78 Attn: Library
79 J. Orcutt

Woods Hole Oceanographic Institution
86-95 Water Street
Woods Hole, MA 02543

80 Attn: J. Lynch

Distribution List for ARL-TR-92-29 under Contract N00039-91-C-0082, TD No. 01A1030 (cont'd)

Copy No.

Department of Ocean Engineering
Massachusetts Institute of Technology
Cambridge, MA 02139
81 Attn: I. Dyer
82 A. Baggeroer

Rosenteil School of Marine and
Atmospheric Science
The University of Miami
10 Rickenbacker Causeway
Miami, FL 33149
83 Attn: H. DeFarrari

The University of Miami
10 Rickenbacker Causeway
Miami, FL 33149
84 Attn: F. Tappert

Department of Electrical Engineering
Polytechnic Institute of New York
Farmingdale, NY 11735
85 Attn: L. B. Felsen

Department of Geology and Geophysics
Geophysical and Polar Research Center
Lewis G. Weeks Hall for Geological Sciences
The University of Wisconsin, Madison
1215 W. Dayton Street
Madison, WI 53706
86 Attn: C. S. Clay

Bolt, Beranek, and Newman
1300 North 17th Street
Arlington, VA 22209
87 Attn: M. Flicker

Bell Telephone Laboratories, Inc.
P.O. Box 496
Whippany, NJ 07981-0903
88 J. Eickmeyer
89 R. Patton

Distribution List for ARL-TR-92-3 under Contract N00039-91-C-0082, TD No. 01A1030 (cont'd)

<u>Copy No.</u>

	The Mitre Corporation 7525 Colshire Drive McLean, VA 22102
90	Attn: K. Hawker
	ORINCON 1755 Jefferson Davis Highway Arlington, VA 22202
91	Attn: H. Cox
	Science Applications International Corporation 1710 Goodridge Drive McLean, VA 22101
92	Attn: C. Spofford
93	J. Hanna
94	R. Cavanagh
	TRW, Inc. TRW Defense and Space Systems Group Washington Operations 7600 Colshire Drive McLean, VA 22101
95	Attn: R. Brown
96	L. Thorne
97	Environmental Sciences Group, ARL:UT
98	Hans A. Baade, ARL:UT
99	Nancy R. Bedford, ARL:UT
100	Mary Beth Bennett, ARL:UT
101	Glen E. Ellis, ARL:UT
102	Karl C. Focke, ARL:UT
103	Richard A. Gramann, ARL:UT
104	David E. Grant, ARL:UT
105	David P. Knobles, ARL:UT
106	Robert A. Koch, ARL:UT
107	Thomas N. Lawrence, ARL:UT

Distribution List for ARL-TR-92-29 under Contract N00039-91-C-0082, TD No. 01A1030 (cont'd)

Copy No.	
108	Scott J. Levinson, ARL:UT
109	Fredrick W. Machell, ARL:UT
110	Peter E. McCarty, ARL:UT
111	Elizabeth L. Miller, ARL:UT
112	Stephen K. Mitchell, ARL:UT
113	Thomas G. Muir, ARL:UT
114	Susan G. Payne, ARL:UT
115	Clark S. Penrod, ARL:UT
116	Timothy M. Scoggins, ARL:UT
117	Carol V. Sheppard, ARL:UT
118	Jack A. Shooter, ARL:UT
119	Steven A. Stotts, ARL:UT
120	Evan K. Westwood, ARL:UT
121	Library, ARL:UT
122	Reserve, ARL:UT